Abstract for the 29th Intl Workshop on Water Waves and Floating Bodies, Osaka (Japan), March 30−April 02, 2014

Numerical Simulation of Fluid-Structure Interaction by an Adaptive Cartesian-Grid CIP Method

by Guanghua He* and Masashi Kashiwagi

Department of Naval Architecture and Ocean Engineering, Osaka University, Osaka, Japan
E-mail: *he@naoe.eng.osaka-u.ac.jp*

1. Introduction

Violent Fluid-Structure Interaction (FSI) is one of the most challenging problems in computational engineering. Due to its extreme nonlinearity (e.g. wave breaking, splitting, merging and air-entrainment), most of the traditionally numerical approaches based on the potential theory are invalid. The Computational Fluid Dynamics (CFD) method is a promising tool to analyze these extremely-nonlinear FSI problems. The CIP (Constrained Interpolation Profile) method [5] is a powerful CFD method for FSI analysis. Hu and Kashiwagi [2, 3] have developed a stationary Cartesian-grid CIP code for extremely-nonlinear FSI.

Recently, an adaptive Cartesian-grid CIP method is proposed by He [1] to save CPU-time and capture the boundaries/interfaces accurately. This adaptive grid moves simultaneously in parallel in each direction to treat the region of violently-varied flows according to a monitoring function. The algorithm is simple, and the computation of spatial derivatives is efficient. It is a grid-regeneration scheme, but the additional CPU-time for this scheme is trivial, since only a single interpolation process is needed for both calculation of the advection process and estimation of values at the new grid point from the old grid point.

This adaptive grid approach has been validated by problems of violent free-surface flows in He [1], however interaction with object/structure has not been studied. It is extended to violent FSI problems in the present study, while the motion of structure is not considered for simplicity.

2. Numerical Theory

The adaptive Cartesian-grid CIP method for the present computations is summarized in this section. The details of the adaptive grid and stationary grid for the CIP method can be found in He [1] and Hu and Kashiwagi [2], respectively.

2.1 Flow Solver

We consider a viscous and incompressible flow. The governing equations for the fluid velocity u_i in the ith direction and the pressure p can be expressed as follows:

$$\frac{\partial u_i}{\partial x_i} = 0 \tag{1}$$

$$\frac{\partial u_i}{\partial t} + u_j \frac{\partial u_i}{\partial x_j} = -\frac{1}{\rho}\frac{\partial p}{\partial x_i} + \frac{1}{\rho}\frac{\partial}{\partial x_j}(\mu S_{ij}) + f_i\,, \tag{2}$$

where $S_{ij} = (\partial u_i/\partial x_j + \partial u_j/\partial x_i)$; ρ is the density of fluid; u_i $(i = 1, 2, 3)$ is the velocity component; and f_i in Eq. 2 denotes the body force, such as the gravity force. No turbulence model is introduced here.

In order to apply the CIP schme, time evaluation of Eq. 2 is performed by a fractional step method. The calculation of equation is divided into an advection step and two nonadvection steps as follows:

$$\frac{u_i^* - u_i^n}{\Delta t} = u_j^n \frac{\partial u_i^n}{\partial x_j} \tag{3}$$

$$\frac{u_i^{**} - u_i^*}{\Delta t} = \frac{1}{\rho}\frac{\partial}{\partial x_j}(\mu S_{ij}^*) + f_i \tag{4}$$

$$\frac{u_i^{n+1} - u_i^{**}}{\Delta t} = -\frac{1}{\rho}\frac{\partial p^{n+1}}{\partial x_i} \tag{5}$$

As mentioned above, Eq. 3 is the advection step, which is solved by the CIP method. The pressure-velocity coupling is treated in a non-advection step calculation, in which the following Poisson equation is solved,

$$\frac{\partial}{\partial x_i}\left(\frac{1}{\rho}\frac{\partial p^{n+1}}{\partial x_i}\right) = \frac{1}{\Delta t}\frac{\partial u_i^{**}}{\partial x_i}\,. \tag{6}$$

Equation 6 is valid for liquid, gas and solid phases. Once Eq. 6 is solved, the distribution of pressure in the whole computation domain can be obtained.

We treat FSI problem as a multiphase problem, which includes three phases (liquid, gas and solid). To recognize different phases, a color function ϕ_m is introduced. In the present work, suffix m denotes 1:liquid, 2:gas and 3:solid phase. A computational cell is defined as $\phi_1 = 1.0$ liquid cell, $\phi_2 = 1.0$ gas cell, and $\phi_3 = 1.0$ solid cell. For each cell, it has the relation of $\sum \phi_m = 1.0$. Once the color function for all phases is determined, the physical properties q (e.g. viscosity, density, pressure) for each computational cell can be calculated by $q = \sum_{m=1}^{3} \phi_m \, q_m$.

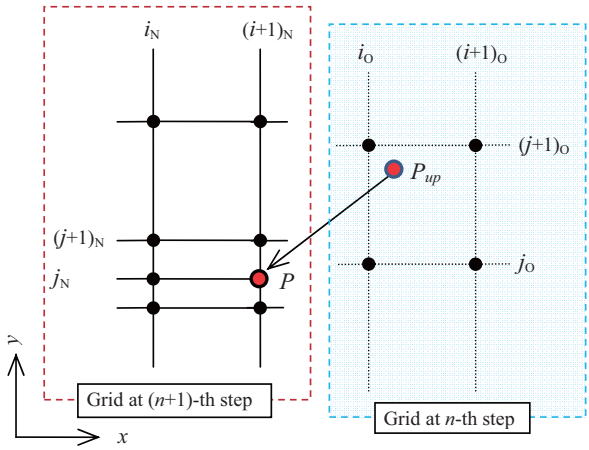

Fig. 1 Definition of an adaptive Cartesian grid.

2.2 Adaptive Cartesian-Grid CIP Method

Firstly, the CIP method [5] for solving the advection process is summarized. Then, the adaptive Cartesian-grid CIP approach [1] is described. A one-dimensional advection equation is used to describe the CIP method,

$$\frac{\partial r}{\partial t} + u\frac{\partial r}{\partial x} = 0\,, \tag{7}$$

where r denotes physical property such as viscosity, density and pressure. This equation represents a translational motion of a wave with velocity u. The CIP scheme shows a different way from the conventional high-order schemes to reconstruct the profile inside a grid cell. The principle concept of the CIP method is that the value r and its spatial derivative $q \equiv \partial r/\partial x$ are used together to construct a cubic polynomial to approximate the profile between two neighbouring grid points.

By differentiating Eq. 7 with respect to x, we obtain the following equation,

$$\frac{\partial q}{\partial t} + u\frac{\partial q}{\partial x} = -\frac{\partial u}{\partial x}q\,. \tag{8}$$

The advection parts in Eqs. 7 and 8 are solved by the CIP method as follows,

$$r_i^{n+1} = R^n\,(x_i - u_i\Delta t) \tag{9}$$

$$q_i^{n+1} = Q^n\,(x_i - u_i\Delta t)\;, \tag{10}$$

where superscripts n and $n+1$ denote the nth and $(n+1)$th time step, respectively; subscript i means the ith grid point; R^n and Q^n are the interpolation approximations to r^n and q^n, respectively. The profile between grid points at the time step $(n+1)$ is determined by shifting the profile with $-u\Delta t$. In other words, to calculate the value of grid point at the time step $(n+1)$ is to find its upstream point at the time step n. This process has no mater with where the grid point (at the time step $(n+1)$) is located. Based on this characteristic of the CIP method, a novel adaptive grid has been proposed by He [1].

The basic concept of this adaptive grid system is simple, efficient, and easy to extend to three-dimensional problem. Figure 1 shows the schematic diagram of this adaptive grid approach. The straight lines paralleled to x- or y-direction move in parallel. '*Old grid point*' (i_O, j_O) and '*New grid point*' (i_N, j_N) in Fig. 1 indicate the grid points at the nth and $(n+1)$th time step, respectively. They are completely independent and the grid number at each time instant can be variable to adapt to the computational solution instantaneously. The procedure of this adaptive Cartesian-grid CIP approach [1] is summarized as follows,

1. New grid points at the next time step are generated to adapt to the computational solution according to a monitoring function. In the present study, the following two-dimensional monitoring function is defined,

$$M(x,y,t)=\sqrt{1+\alpha\left(\left(\frac{\partial\phi}{\partial x}\right)^2+\left(\frac{\partial\phi}{\partial y}\right)^2\right)}+\beta\left(\left|\frac{\partial^2\phi}{\partial x^2}\right|+\left|\frac{\partial^2\phi}{\partial y^2}\right|\right), \tag{11}$$

where α and β are user-defined scaling coefficients to control the level of grid-clustering, and ϕ denotes the flow properties, such as the density, color function, velocity, and so forth. It should be noticed that the monitoring function can be freely defined according to the computed problem.

2. The physical values at the time step $(n+1)$ such as density, velocity and pressure, are then evaluated simultaneously during solving the advection process. Let us take the P grid point (x_{i_N}, y_{j_N}) for example, which is shown in Fig. 1. The value of r^{n+1} in Eq. 9 at this P point is shifted from its upstream point $P_{up}=(x_{i_N}-u_i\Delta t, y_{j_N}-v_i\Delta t)$. P_{up} is easy to interpolated from the neighboring points at the time step n, then the value of P grid-point is obtained.

3. The remaining nonadvection steps, Eqs. 4-6, are solved.

It is important to note that the value-interpolation from the old grid to the new grid is accomplished simultaneously within the advection process, without additional value-mapping from old grid system to new grid system. It is the essential difference to most of re-meshing schemes, which take additional CPU-time due to the value-mapping from old grid to new grid systems.

3. Numerical results

The first validation case is a 2D flow around a stationary square cylinder. The Reynolds number is $Re=\rho UB/\mu=200$, where B is cylinder width, U is the velocity of uniform flow. Snapshots of the adaptive grid at several time instants are shown in Fig. 2. A uniform grid generated at the initial time is shown in Fig. 2(a), and an adaptive finer grid is then generated simultaneously according to the computational solution, as shown in Fig. 2(b, c). It is found that the finest grid is distributed around the body surface. The adaptive grid is generated automatically according to a user-defined monitoring function as shown in Eq. 11. It is clear that the fine grid is generated and distributed for sharply-changing regions and the coarse grid for steady regions.

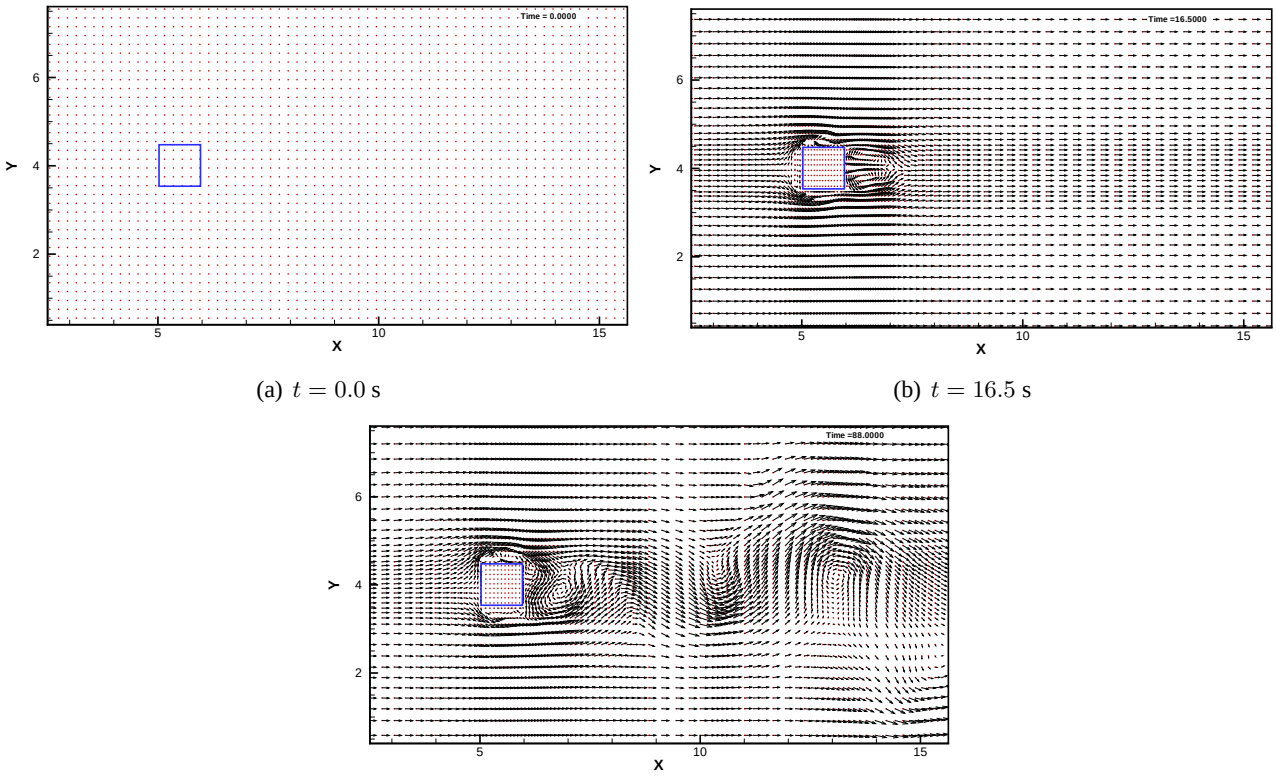

(a) $t=0.0$ s (b) $t=16.5$ s

(c) $t=88.0$ s

Fig. 2 Snapshots of the adaptive grid in the test of a uniform flow flow past a square cylinder.

The second validation case is collapsing water column with an obstacle, which is a more challenging fluid-structure problem with fluid splitting, merging and air-entrainment. The computational conditions are set the same with experimental measurement by Koshizuka et al. [4]. Figure 3 shows snapshots of the adaptive grid at several time instants. It can also been seen that an adaptive finer grid is generated instantaneously according to the computational solution, as shown in Fig. 3. It is also found that the grid becomes insufficient after the water impacting on the right vertical wall. It should be pointed out that no special interface-capturing/tracking scheme is employed in this study.

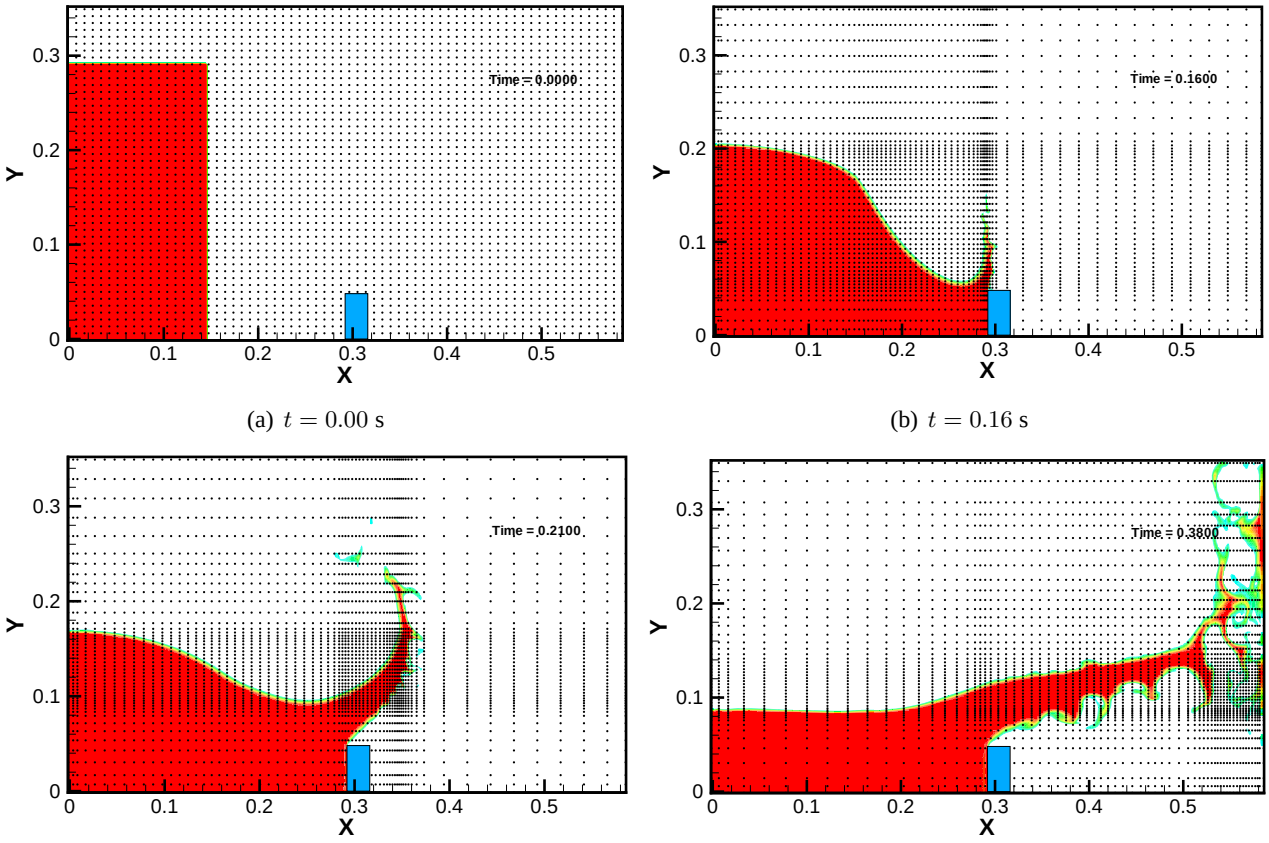

(a) $t = 0.00$ s (b) $t = 0.16$ s

(c) $t = 0.21$ s (d) $t = 0.38$ s

Fig. 3 Snapshots of the adaptive grid in the test of collapsing water column with obstacle.

4. Conclusions and Discussion

A new adaptive Cartesian-grid CIP method was validated by two 2D benchmark tests. One was a uniform flow flow past a square cylinder, the other was collapsing water column with an obstacle. It was confirmed that the adaptive grid is capable of tracing regions with violent flows, and a finer grid is then generated automatically to adapt to the violent changing of the flows. Further study of extending this approach to other violent FSI problem with consideration of motion-free or elasticity is still on the way.

References

[1] Guanghua He. A new adaptive cartesian-grid cip method for computation of violent free-urface flows. *Applied Ocean Research*, 43:234–243, 2013.

[2] Changhong Hu and Masashi Kashiwagi. A cip-based method for numerical simulations of violent free-surface flows. *Journal of Marine Science and Technology*, 9(4):143–157, 2004.

[3] Changhong Hu and Masashi Kashiwagi. Two-dimensional numerical simulation and experiment on strongly nonlinear wavebody interactions. *Journal of Marine Science and Technology*, 14(2):200–213, 2009.

[4] S. Koshizuka, H. Tamako, and Y. Oka. a particle method for incompressible viscous flow with fluid fragmentation. *Comput. Fluid Dyn. J.*, 4(1):29–46, 1995.

[5] T. Yabe and T. Aoki. A universal solver for hyperbolic equations by cubic-polynomial interpolation i. one-dimensional solver. *Computer Physics Communications*, 66(23):219–232, 1991.